

# VALIDATION PROTOCOL APPLIED TO AN AUTOMATIC CO-REGISTRATION METHOD BASED ON MULTI-RESOLUTION ANALYSIS AND LOCAL DEFORMATION MODELS

Philippe Blanc.

Ecole des Mines de Paris, Groupe Télédétection & Modélisation, B.P. 207, F-06904 Sophia Antipolis Cedex.  
Aérospatiale, Service Applications des Systèmes d'Observation, SE/TNE, B.P. 99, F-06156 Cannes la Bocca Cedex.

Lucien Wald.

Ecole des Mines de Paris, Groupe Télédétection & Modélisation, B.P. 207, F-06904 Sophia Antipolis Cedex.

Commission II, Working Group 8.

**KEY WORDS:** automatic co-registration method, multi-resolution analysis, local deformation models, validation protocol.

## ABSTRACT:

The issue of co-registration distortions between images is one of major problems involved in data fusion processes. This conclusion can be extended to change detection generally also performing on a pixel basis. Accurate methods are therefore required for co-registration of images in these particular cases. It is the reason why we present a co-registration method using multi-resolution analysis and local deformation models. This work includes a validation protocol that enables the assessment of the accuracy, the robustness and the quality provided by any co-registration method. This validation protocol has been then applied to the presented method and the results have been compared to those provided by a standard one. According to this validation, this method provides a very fine correction of the geometric distortions that is better than those generally provided by standard co-registration methods. As a conclusion, this method seems to constitute an answer to the need of high quality co-registration as a pre-processing of fusion and change detection processes. Moreover, it is a fully automatic method that potentially enables an operational utilisation of high quality.

## RÉSUMÉ:

Le problème de non-superposabilité des images est un des problèmes majeurs soulevés par les applications de fusion de données. Cette conclusion peut être étendue aux applications de détection des changements mettant aussi généralement en jeu des comparaisons "pixel à pixel". Des méthodes précises sont donc nécessaires pour recalculer les images en amont de telles applications. C'est la raison pour laquelle nous présentons une nouvelle méthode de mise en correspondance géométrique utilisant l'analyse multi-résolution et des modèles de déformations locaux. Ce travail propose de plus un protocole de validation qui permet d'évaluer, dans le cas général, la précision, la robustesse et la qualité d'une méthode de mise en correspondance géométrique. Ce protocole de validation a été appliqué à la méthode présentée et comparée à une méthode standard. D'après cette validation, la méthode présentée permet une correction très fine des décalages géométriques, meilleure que celles généralement obtenues par des méthodes de mise en correspondance standard. En conclusion, cette méthode semble apporter une réponse au besoin de mise en correspondance de très grande qualité pour des prétraitements aux applications de fusion de données ou de détection des changements. Enfin, cette méthode de mise en correspondance est une méthode entièrement automatique, ouvrant ainsi des perspectives d'utilisations opérationnelles de grande qualité.

## 1. INTRODUCTION

Earth observation has reached a high degree of maturity as evidenced by the number and the high variety of thematic applications using remotely sensed images as information sources. To take the best possible use of this variety of information, we have to cope with a large amount of data. Therefore, we have to be able to extract and to produce synthetic information relevant for each specific application. Data fusion techniques constitute a possible answer to enlarge our knowledge of the real world by taking advantage of all the images and data at our disposal.

However, data fusion involves problems, and in particular, "pixel to pixel" fusion processes raise up the issue of geometric co-registration error between the images to merge. Indeed, we have shown and quantified in Blanc *et al.* (1998) that even small geometric distortions (mean and standard deviation of geometric distortions was, in this case, less than respectively 0.3 and 0.1 pixel), have influences in a noticeable manner on the products of « pixel to pixel » fusion processes. This conclusion can be extended to change detection generally also performing on a pixel basis. For example, Townshend *et al.* (1992) have emphasised that the registration accuracy is extremely important for any remote sensing system if reliable detection of land cover change is a major objective.

The aim of this paper is first to present an automatic co-

registration method that is an answer to this need of high quality co-registration as a pre-processing of such fusion processes. Then we present a validation protocol that has been used to assess the effectiveness and the accuracy of this method compared to a standard co-registration method.

## 2. DESCRIPTION OF THE CO-REGISTRATION METHOD

### 2.1 Main principle

The purpose of a co-registration method is to determine the geometric deformation model between two or more images of a same scene. In other words, it consists in estimating, for each pixel of an image, called hereafter the reference image, the corresponding location, generally at a sub-pixel accuracy, in the other images called the work images. The geometric shifts in the column and the line directions between those corresponding pixels are called geometric disparities or distortions between the images.

In this paper, we present a fully automatic co-registration method based on multi-resolution analysis and local geometric distortion model. It is an improved version of the co-registration method published in Djamdji *et al.* (1993, 1995).

The images to co-register are decomposed at different decreasing resolutions by the use of a multi-resolution

analysis. In our work, the multi-resolution analysis is based upon a discrete wavelet transform provided by the «à trous» algorithm. Information about this specific implementation of discrete wavelet transform can be found in Holdshneider *et al.* (1989). At the coarser resolution, couple of corresponding points in the reference and the work images, called hereafter tie points (TPs), are automatically chosen and matched. A first estimation of a geometric deformation model between the images is made by adjustment of the co-ordinates of those TPs. Then, this estimation is iteratively refined till the original resolution using the previous deformation model and the new information in the next finer resolution images.

This method is illustrated in the Figure 1.

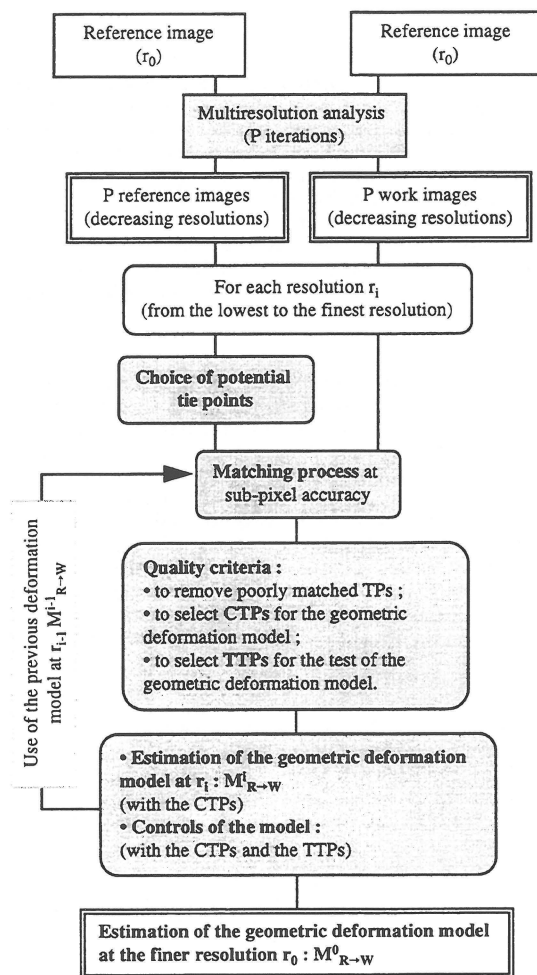


Figure 1: The co-registration method.

This flowchart shows that, for each iteration (*i.e.* for each resolution), this approach relies on four main steps:

- the choice of potential TPs in the reference image ;
- the matching process of those points in the work image to get TPs ;
- the classifying of those TPs according to quality criteria ;
- the estimation and the controls of the geometric deformation model.

All those steps will be presented in this paper.

## 2.2 The choice of potential tie points (potential TPs)

This stage makes a pre-selection among all the pixels of the reference image in order to extract distinctive points at the current resolution. The word "distinctive" means that

those points in the reference image should be localised easily and accurately in the work images at the current resolution provided that they are in their swath.

We assume that those distinctive points lie on important transitions at the current resolution. Therefore, they are considered to be local maxima of significant structure detected in the wavelet coefficients thanks to a threshold transform. In order to have a dense and homogeneous distribution of those points, we chose automatically a local threshold proportional to local standard deviations of the wavelet coefficients. A second threshold, proportional to the standard deviation of the whole image of wavelet coefficients is done to eliminate points extracted in homogeneous regions on account of the noise.

## 2.3 The matching process of potential TPs

The aim of the matching process is to localise accurately, in the work image, the potential TPs. Therefore, from this list of potential TPs, this process provides a list of TPs between the images to co-register.

Let us consider a potential TP. The previous deformation model provides a first estimation of its location in the work image. From this first estimation, a new search is made to refine it at the current resolution. The extend of the search area depends on the current resolution and on an error overestimation of the previous deformation model. For each pixel of this search area in the work image, is computed a similarity measurement with the point in the reference image. In our case, the similarity measurement is based upon the normalised correlation coefficient between two context windows centred respectively on the two points. There is a compromise for the size of those context windows. Indeed, those windows have to be large enough to constitute good information contexts for the points to compare but not too large to prevent the estimation of the location from being too smoothed. A matrix of similarity measurement for each pixel of the search area is then obtained. A bicubic interpolation and a standard method of maximisation of function applied to this matrix provide the location, at a sub-pixel level, of its maximum when it exists and is unique.

Despite the pre-selection made by the choice of the potential TPs, the matching process provides an estimation of the geometric disparities with an error and even, for some potential TPs, is not able to provide it. The success and the accuracy of the matching process depends first on the quality of the mutual information of the context windows that have to be representative and stable (according to the measure of similarity) between the two images. It also depends on the robustness of the similarity measurement facing the apparent variability between the images to co-register. More information about matching process in a theoretical and practical point of view can be found in Leclerc (1987).

## 2.4 The sorting of the TPs

The error of the matching process is not constant and depends on many unknown and hidden parameters specific to each TP. Nevertheless, the purpose of this stage is to be able to create a sub-set of a given number  $n$  of elements (less than  $N$ , the number of TPs after the matching process) made up of the "best"  $n$  TPs as far as accuracy of matching is concerned. This sorting is all the more selective as  $n$  is less than  $N$ .

In order to select those "best"  $n$  TPs that will belong to this new sub-set, some quality criteria of the matching process for each TP are used. More precisely, we chose five criteria that are supposed to test the robustness of the matching and to filter them:

- the index proposed in Moravec (1977) that measures the presence and the intensity of structures in the context windows ;
- the value of the maximum, at sub-pixel level, reached

- by the similarity measurement ;
- the ratio between the maximum and the mean of the similarity matrix ;
- the ratio between the maximum and the second maximum in its neighbourhood (8-connexity) reached by the similarity measurement ;
- a measure of the isolation of each TP among the others in the reference image.

All those criteria are not comparable to each other. Therefore, to take them all into account for the selection, a "normalisation" has been applied, based upon the rank order of the TPs for each criterion. A synthetic criterion is then obtained by making a weighted average of the five rank orders for each TP. The weight associated to a criterion is related to its importance for the filtering. The selection of the "best"  $n$  TPs is then assumed to correspond to the selection of the best  $n$  TPs considering this synthetic criterion. It is important to note that this sorting does not proceed to an estimation of the matching error for each TPs but only to a classification of their relative matching quality thanks to those criteria.

Of course, other criteria can be taken into account for the classifying. For example, the acquisition parameters can be used to evaluate a likelihood measurement of the disparities for each TP.

From those  $n$  selected TPs, are extracted a relatively small number (about 10%) that will not be used for the estimation of the geometric deformation model but will have an important part, described in §2.6, for the test of this model. Those TPs, called hereafter TTPs (Test TPs) are randomly chosen so that there is a homogeneous distribution in the reference image. The rest of TPs, called hereafter CTPs (Construction TPs), will be used as data to estimate the geometric model. Therefore, we have :

- a set of  $n_c$  CTPs :

$$S_C = \{CTP_k: (x_{R,k}^C, y_{R,k}^C) \rightarrow (x_{R,k}^C, y_{R,k}^C)\}_{k \in [1, n_c]} ;$$

- a set of  $n_t$  TTPs :

$$S_T = \{TTP_k: (x_{R,k}^T, y_{R,k}^T) \rightarrow (x_{R,k}^T, y_{R,k}^T)\}_{k \in [1, n_t]} ;$$

where  $n = n_t + n_c$  et  $n_t \approx n/10$ .

## 2.5 The estimation of geometric distortion model

The geometric distortion model is in fact a mathematical function that gives, for each pixel of the reference image, the estimation of the geometric disparities with the work images:

$$M_{R \rightarrow W} : P_R = (x_R, y_R) \rightarrow M_{R \rightarrow W}(P_R) = (dx, dy)$$

For each pixel of the reference image, the corresponding location in the work image is

$$(x_W = x_R + dx, y_W = y_R + dy) \\ \text{where}$$

$$(dx, dy) = M_{R \rightarrow W}(x_R, y_R)$$

This model is in fact an interpolation of the geometric disparities measured in the sub-set  $S_C$ . This interpolation consists in choosing an analytic function with some parameters and in adjusting them in order to fit this function to the set of geometric disparities  $\{d_k^C = P_{W,k}^C - P_{R,k}^C\}_{k \in [1, n_c]}$  at the corresponding location in the reference image. The number of parameters is the degree of freedom of the geometric distortion models and divides them into two categories: global and local models.

Degrees of freedom of *global deformation models* are significantly less than the number of CTPs. It can only reproduce the trend, the "low frequency" of the geometric disparities measured at the location of the CTPs. In other words, global models generally do not fit to the CTPs and the differences are all the more important as the complexity of the actual field of geometric disparities is important and "greater" than the degree of freedom of the models. For example, a second order polynomial model is a global model because it has a degree of freedom equal to six and is generally fitted to a set of significantly more than six CTPs by minimising the mean square error.

On contrary, the degree of freedom of a *local deformation model* is almost equal to the number of CTPs. Unlike the

global models, the local ones present the possibility to take into account, locally, the disparity measured on each CTP. The quality of a local model is extremely dependent on the accuracy of the matching of each CTP and on density and the homogeneity of the distribution of the CTPs.

Two types of local deformation models are used in our co-registration method:

- local models based upon interpolation functions defined in "one single block"*. The thin plate interpolation described in Lemehaute (1989) belongs to this type. This technique provides a local geometric deformation model that has a parameter controlling the degree of firmness of the thin plate function. This parameter can be computed thanks to a cross-validation method in order to enable the geometric deformation model to filter errors in the given disparities of the CTPs. The thin plate interpolation has an other advantage: it provides a deformation model that is stable far from the CTPs. Nevertheless, on account of the time of computation, this technique is limited by the number of CTPs that has to be less than 600 ;

- local models based on piecewise interpolation functions*. As the distribution of the CTPs in the reference image is not generally regular, the piecewise functions is be defined on a Delaunay triangulation (see Watson, 1981). The simplest piecewise interpolation method is based upon polynomials of degree 1 provides continuous geometric deformation model whose derivatives are not continuous. A more accurate, and more complex, method called Heigh-Clough-Tucher method is based upon polynomials of degree 3 (Lemehaute, 1989). It makes use locally thin plate interpolation method and provides a continuous geometric deformation model but whose derivatives are also continuous. In practice, those interpolation methods are not limited by the number of CTPs but can not be computed out of their convex hull. To cope with this limitation, they can be completed by the use of other interpolation methods that can be computed at each pixel (e.g. polynomial or thin plate deformation model).

## 2.6 The quality control of the geometric deformation model

At this point of the treatment, and at the current resolution, two types of control are applied to test the geometric deformation model  $M_{R \rightarrow W}$ .

The first control consists in comparing statistically (bias, standard deviation, etc.) the disparities  $d_k^C = P_{W,k}^C - P_{R,k}^C$  measured at each CTP and the modelled (interpolated) disparities  $M_{R \rightarrow W}(P_{W,k}^C)$ . As those disparities have been used to estimate the geometric deformation model, this comparison gives information about the *quality of the interpolation* as far as the given data are concerned. For example, this comparison is useful to check the quality of a polynomial model and to find the degrees of the two polynomials that minimise the error of the interpolation.

The second control consists in comparing the disparities  $d_k^T = P_{W,k}^T - P_{R,k}^T$  measured at each TTP and the modelled (interpolated) disparities  $M_{R \rightarrow W}(P_{W,k}^T)$ . It is important to note that those data have not been used to estimate the geometric deformation model but could have been. Therefore, this comparison is a sort of "blind test" that enables a control of the *relevance* of the choice of the analytic functions and their parameters to model the actual field of disparities measured by the matching process.

The estimation of the deformation model can be judged satisfactory when the differences in the two controls are statistically small and comparable.

As a conclusion, those two controls are only meant to test the quality of the geometric deformation model in terms of errors and relevance of the interpolation but do not provide an estimation of the co-registration error. This estimation would require an estimation of the matching error that seems to be very hypothetical.

### 3. GENERAL ASSESSMENT PROTOCOL OF A CO-REGISTRATION METHOD QUALITY

#### 3.1 The protocol

We propose here a protocol that enables the assessment of the accuracy, the robustness and the quality provided by a co-registration method in a realistic and totally controlled case.

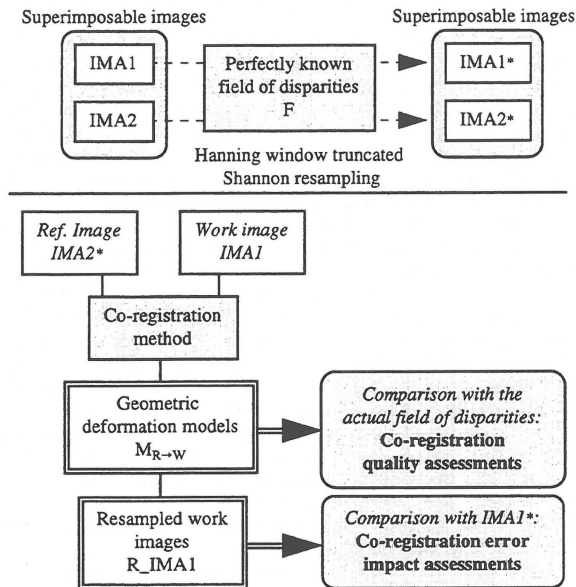


Figure 2: Assessment protocol of a co-registration method quality.

The following approach, illustrated in Figure 2, is proposed: let us consider two superimposable images IMA1 and IMA2 and a field of geometric disparities  $F$  that is perfectly known for each pixel of the two images. Those images are then re-sampled into new images IMA1\* and IMA2\*, thanks to a re-sampling method (e.g. Hanning window truncated Shannon re-sampling), by injecting the field of geometric disparities  $F$ . In other words, we synthesised new images IMA1\* and IMA2\* radiometrically identical to the original image but with perfectly known geometric disparities between them. In order to have a realistic and representative validation, the field  $F$  should be complex, spatially variable and non analytic.

The co-registration method, which quality has to be assessed, is applied to IMA2\* as the reference image and IMA1 as the work image. It provides, at the finest resolution, a geometric deformation model  $M_{R \rightarrow W}$ . This model is then used to re-sample IMA1 into a new image  $R\_IMA1$ . Ideally,  $M_{R \rightarrow W}$  and  $R\_IMA1$  should be exactly equal respectively to the field  $F$  and to IMA1\*.

Therefore two types of comparison are possible that enable two types of quality assessment:

- the comparison between the geometric deformation model and the actual field of disparities gives information about the *co-registration quality itself* ;
- the comparison between the original image IMA1\* and  $R\_IMA1$  gives information about the *impact of the co-registration error* on the re-sampled image.

Those two types of quality assessment are now discussed.

#### 3.2 Co-registration quality assessment

As the geometric disparities between IMA1 and IMA2\* is perfectly known at each pixel, we can accurately measure, for each pixel, the co-registration error. Some statistic

criteria are proposed to describe globally the differences between the actual and the estimated disparities in the line and in the column directions. For one given direction, are proposed:

- *the bias*: it is the mean, in pixel, of the difference between the disparities. The closer to zero, the more similar the disparities are ;
- *the difference of variances* (variance of the actual disparities minus the variance of the estimated ones) and its relative value to the variance of the actual disparities. This value is a measure, to some extent, of the quantity of information added or lost by the estimation. For an estimation that provides too much information (information may be noise or artefacts) the difference is negative. In the opposite case, this value is positive. Ideally, this difference should be nil ;
- *the coefficient of correlation* between the actual and the estimated disparities shows their spatial similarity in shape. It should be as close to 1 as possible ;
- *the standard deviation of the difference*, globally indicates the level of estimation error in pixel. Ideally, it should be null.

#### 3.3 Co-registration error impact assessment

As they have both been re-sampled by the same interpolation kernel, the differences between  $R\_IMA1$  and IMA1\* are only due to the residual geometric disparities after the co-registration process. It is the reason why the comparison between those two images that should be perfectly identical is a roundabout way to assess the quality of the co-registration method. This comparison is achieved with the comparison criteria of two images proposed as part of a quality assessment of fusion of satellite images of different resolution described in Wald *et al.* (1997).

Those two images can also be used for an other quality assessment based on visual inspection. This assessment consists in visualising rapidly the two images alternately. On account of the persistence of vision, one can visually estimate the local residual geometric disparities.

### 4. QUALITY ASSESSMENT AND VALIDATION RESULTS

In order to assess the accuracy, the robustness and the quality of the co-registration provided by the presented co-registration method we have applied the assessment protocol described in §3 to a favourable and a less favourable cases:

- the two images to co-register are identical. In this case,  $IMA1 = IMA2$  ;
- the two images to co-register are not identical. In this case,  $IMA1 \neq IMA2$ .

In order to have a reference, both quality assessments of the presented co-registration have been achieved in comparison with the results provided by a standard method.

Before presenting those results, we present the co-registration method that we chose as a standard one and the data that have been used for the different assessments/validations.

#### 4.1 The standard co-registration method

We chose as a standard co-registration method, a broadly used manual one. This method consists in choosing points as uniformly distributed as possible in the reference image and matching them manually in the work image. In order to have a sub-pixel accuracy in the manual matching process, the work image have been over-sampled four times. The number of TPs is limited by the manual acquisition and is generally less than 100. Those TPs are then used in order to estimate a polynomial geometric deformation model (generally of degrees two).



## 4.2 Data for the different assessments/validations

In this paper, we deal with a 100 km<sup>2</sup> sub-region extracted from a SPOT multispectral XS image (resolution: 20 m) and the corresponding SPOT panchromatic P (resolution: 10 m) of the city of Barcelona.

The three channels of the multispectral image XS are supposed to be perfectly superimposable. Those images have then been re-sampled with the Hanning window truncated Shannon interpolation into new images by injecting a realistic, non analytic and complex field of geometric disparities.

In order to get this field, the technique of sub-pixel matching described in §2.3 has been performed to localise *each pixel* of XS1 in the P image degraded to 20 m. After filtering the poorly matched points, a field of very small but complex and realistic geometric disparities was obtained. In our opinion, this geometric distortion is due to the small difference in the acquisition parameters (angle along the track) for the panchromatic and the multispectral modes. This difference induces geometric distortions like translation, zoom and parallax effects. Therefore, the field of small geometric distortions that have been extracted is, in fact, the residual geometric disparities that have not been totally corrected by the co-registration method applied to make the P and the XS images superimposable. It is important to note that the field have been multiplied by four to have a more consequent field of geometric disparities for the sake of the different assessment/validations. Table 3 shows the minima, the maxima, the mean and the standard deviation of this injected field of disparities. Figure 4 displays the field of disparities respectively in the line directions. One can note that this field exhibits complex spatial structures which seems to be correlated to orographic features of the scene.

	$\Delta x$	$\Delta y$
Mean	-1.05	1.11
Standard deviation	0.35	0.41

Table 3: Minima, maxima, means and standard deviations in pixel of the geometric disparities field in column and line direction (respectively  $\Delta x$  and  $\Delta y$ ).

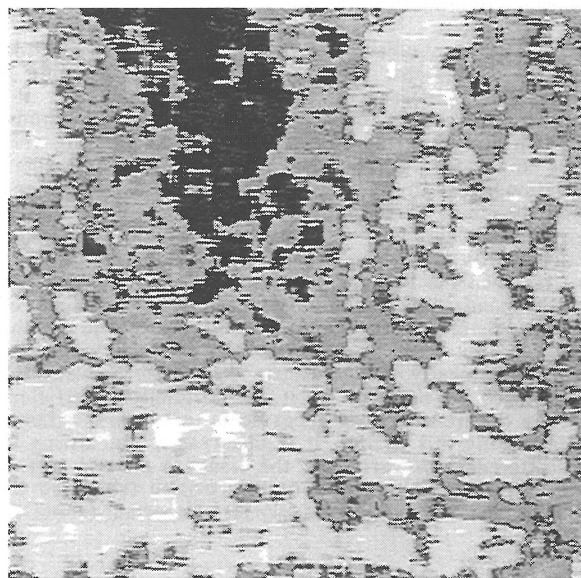


Figure 4: Field of geometric disparities in the line direction.



(a)



(b)

Figure 5: (a) Sub-region of the original XS1 image. (b) Same but for the XS3 image.

For the sake of clarity, we only consider the spectral bands XS1 and XS3 of the SPOT multispectral image (see Figure 5). The re-sampled images are called hereafter respectively XS1\* and XS3\*.

## 4.3 Quality co-registration with XS1 and XS1\*

In this case, we applied the assessment protocol with IMA1=IMA2=XS1 to the presented and the standard methods.

**4.3.1 Facts of the standard co-registration:** 33 CTPs have been manually selected. The mean distance between two CTPs is about 75 pixels. The geometric deformation model, whose disparities in the line direction are illustrated in Figure 7 (a), is based on a polynomial of degree 2 interpolation method.

**4.3.2 Facts of the presented co-registration:** at the finest resolution, the matching process provides 2545 TPs. As

this case is a favourable one for the matching process, the sorting process has not been chosen very selective: from those TPs have been selected 1380 CTPs and 170 TTPs. The mean distance between two CTPs is about 11 pixels and about 33 pixels for the TPs. As there is a great number (greater than 600) of CTPs, the geometric deformation model, illustrated for the line direction in Figure 7 (b), is based on the Hsieh-Clough-Tocher piecewise interpolation method.

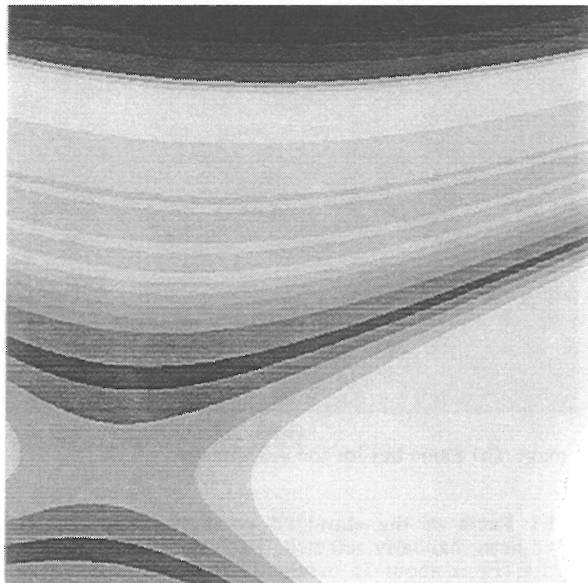
**4.3.3 The compared results of the co-registration quality assessment:** the statistical criteria in Table 6 describe the differences between the actual and the estimated disparities for the two co-registration methods. One can note that, for both methods, the biases are very close to the ideal value. It is also true for the standard deviations: less than 7.2 m for the standard method and less than 3.6 m for the presented one. According to those two criteria, the presented method provides a slightly better quality of co-registration. Nevertheless, the quality gap between the two methods is small. Indeed, the bias and the standard deviation only provide a "global view" of the co-registration errors and, therefore, do not reveal the ability or not of each co-registration method to correct finely and locally the geometric disparities between the two images. To make up for it, the correlation coefficient and the difference of variances seem to be more suitable for assessing this ability. It is observable that, owing to the differences of variances, the standard method suffers from a very important lack of information (about 80 %) whereas this lack is distinctively less important (about 10

%) for the presented one. The same remark can be done as far as the lack of shape similarity (correlation) between the actual field and the deformation model is concerned. This superiority of the presented co-registration method, also visible by the comparison of Figures 7 (a) and 7 (b) with Figure 4, was foreseeable: thanks to the local deformation model supported by the great number of CTPs, the presented method provide a very finer and more accurate geometric correction than the standard method with its polynomial of degree two model estimated by 33 CTPs.

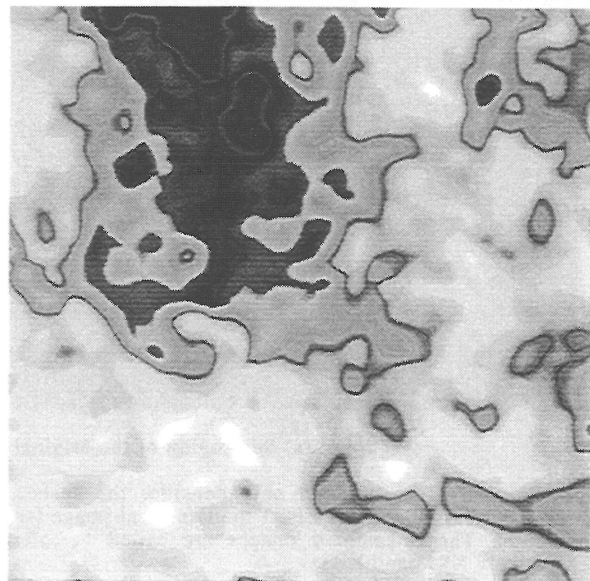
**4.3.4 The compared results of the co-registration error impact assessment:** the quality of the two co-registration methods can be firstly analysed and compared by the visual inspection of XS1\* and R\_XS1 alternatively as described in §3.3. It is observable that the standard method has globally corrected the geometric disparities but local residual disparities obviously still remain, that degrade the co-registration quality. On the contrary, the inspection shows that the presented method provide a local and accurate geometric correction. The statistical criteria for the comparison of XS1\* with R\_XS1 in Tables 8 and 9 corroborate the visual inspection and show that, in term of co-registration error impact, the presented method is clearly better than the standard one. It is interesting to note that the comparison between the two images, and especially the cumulative error histogram, is extremely sensitive to the co-registration quality.

		$\Delta x$	$\Delta y$
<b>Standard method</b>	Bias (ideal: 0)	0.11	0.00
	Standard deviation (ideal: 0)	0.31	0.36
	Correlation (ideal: 1)	0.59	0.47
	Difference of var. in percent (ideal: 0)	95.6 %	77.9 %
<b>Presented method</b>	Bias (ideal: 0)	0.01	0.02
	Standard deviation (ideal: 0)	0.15	0.18
	Correlation (ideal: 1)	0.90	0.90
	Difference of var. in percent (ideal: 0)	9.5 %	13.7 %

Table 6: Means, standard deviations in pixel for the error of the standard and the presented co-registration methods in the column and row directions (respectively  $\Delta x$  and  $\Delta y$ ). Correlation and difference of variances are also reported.



(a)



(b)

Figure 7: (a) Geometric deformation model in the line direction provided by the standard method. (b) Same but for the presented method.

	Bias (ideal: 0)	Standard deviation of the difference (ideal: 0)	Correlation coefficient (ideal: 1)	Difference of variances (ideal: 0)
<b>Standard method</b>	0.00 0.0 %	3.3 4.6 %	0.971	-0.36 -0.2 %
<b>Presented method</b>	0.00 0.0 %	1.6 2.2 %	0.993	-0.01 -0.06 %

Table 8: Statistical criteria (bias, difference of variances, correlation coefficient and standard deviation of the difference) in digital counts for comparison between XS1\* and the re-sampled images R\_XS1 for the two methods.

	0.001	1	2	5	10	20
<b>Standard method</b>	27	28	58	85	97	100
<b>Presented method</b>	47	48	83	97	100	100

Table 9: Probability (in percent) for having in a pixel a relative error less than or equal to the thresholds noted in the first row for the comparison between XS1\* and the re-sampled images R\_XS1 for the two methods. The ideal value is 100 as early as the first threshold 0.001 %.

#### 4.4 Quality co-registration with XS1 and XS3\*

In this case, we applied the assessment protocol with IMA1=XS3 and IMA2=XS1 to the presented and the standard methods. On account of the difference of the spectral bands of XS1 and XS3, the two images are not identical (correlation coefficient is equal to 0.34).

**4.4.1 Facts of the standard co-registration:** only 21 reliable CTPs have been manually selected between the images. The mean distance between two CTPs is about 78 pixels. The geometric deformation model is based on a polynomial of degree 2 interpolation method.

**4.4.2 Facts of the presented co-registration:** this case is less favourable than in §4.3 for the automatic matching based on correlation coefficient. It is the reason why, at the finest resolution, the matching process provides only 1070 TPs. We decided to be more selective in the sorting of TPs: from those TPs have been selected 200 CTPs and 40 TTPs. The mean distance between two CTPs is about 28 pixels and about 60 pixels for the TPs. As there is a relatively small number of CTPs, the geometric deformation model is based on the thin plate interpolations method whose firmness parameter is equal to 0.

**4.4.3 The compared results of the co-registration quality assessment:** according to the statistical criteria in the Table 10, the presented method still provides the best co-registration quality even if the gap between the two compared methods is smaller than in the more favourable previous case. Moreover, one can note that, compared this previous case, the standard deviation (less than 5.8 m), the correlation coefficient (0.73) and the difference of variances (24 %) show that the presented method suffered from a lack of CTPs to rectify accurately and locally with the same efficiency. This lack of CTPs is due to the fact that the images to co-register are poorly correlated and that the sorting process has been chosen very selective in order to be sure of the matching accuracy of the selected TPs.

**4.4.4 The compared results of the co-registration error impact assessment:** those results in Tables 11 and 12 corroborate the previous results: even if the presented method provide better result, the co-registration quality are globally degraded on account of the differences of the two images to co-register. Nevertheless, the quality provided by the presented co-registration in this unfavourable case is better than the quality provided by the standard method in the favourable case.

		$\Delta x$	$\Delta y$
<b>Standard method</b>	Bias (ideal: 0)	0.08	0.13
	Standard deviation (ideal: 0)	0.38	0.34
	Correlation (ideal: 1)	0.08	0.57
	Difference of var. in percent (ideal: 0)	89.6 %	76.4 %
<b>Presented method</b>	Bias (ideal: 0)	-0.06	0.07
	Standard deviation (ideal: 0)	0.24	0.29
	Correlation (ideal: 1)	0.73	0.72
	Difference of var. in percent (ideal: 0)	23.8 %	20.6 %

Table 10: As Table 6, but for the co-registration of XS1 and XS3\*.

	Bias (ideal: 0)	Standard deviation of the difference (ideal: 0)	Correlation coefficient (ideal: 1)	Difference of variances (ideal: 0)
<b>Standard method</b>	-0.11 0.2 %	5.54 7.9 %	0.940	9.8 3.8 %
<b>Presented method</b>	0.00 0.0 %	4.2 6.0 %	0.966	-0.3 -0.12 %

Table 11: As Table 8, but for the co-registration of XS1 and XS3\*.

	0.001	1	2	5	10	20
<b>Standard method</b>	23	23	51	78	93	99
<b>Presented method</b>	29	29	61	86	96	99

Table 12: As Table 9, but for the co-registration of XS1 and XS3\*.

## 5. CONCLUSION

We have presented a fully automatic co-registration method that allows an estimation of the geometric disparities between two images of a same scene. This method makes use of a multi-resolution analysis as described in (Djamdj, 1995) and local deformation models.

This work also proposes a formal assessment protocol that provides two types of data that enable different and complementary quantitative assessments and validations of a co-registration method in realistic and totally controlled cases:

- this protocol provides for each pixel of the reference image the "right" error made by the tested co-registration method. This enables a straight quality assessment by appraising the co-registration error ;
- it also provides two supposed superimposable images whose differences are solely due to residual co-registration error of the tested method. Those data enable a roundabout quality assessment by appraising the impact of the co-registration error.

Both types of quality assessment are based upon visual and different statistical criteria that describe the quality of the co-registration method. As far as statistical criteria are concerned, it is important to note that the bias and the standard deviation in the straight quality assessment are not totally adequate to assess the ability of the tested method to co-register finely and locally. Other statistical criteria of the residual geometric disparities (correlation coefficient, difference of variances) or the visual inspection and the comparison of images as described in (Wald *et al.*, 1997) in the roundabout quality assessment are therefore required to assess accurately the quality of the tested method.

This assessment protocol has been applied to our co-registration method with two identical images (favourable case) and with two different images (unfavourable case). Those quality assessments have been compared to those provided by a generally used manual co-registration method. This study has shown that our method provides, in each case, better result as far as global and local accuracy of co-registration are concerned. Nevertheless, one can note that the quality gap between the proposed method and the standard one is relatively small in the unfavourable case. We emphasise that the validation protocol has been applied on a small sub-scene (512x512). In an operational use, the images to co-register are generally definitely larger (e.g. a SPOT XS image is about 3000x3000 pixels). In this context, the standard method that makes use of a polynomial deformation model based on a small number of CTPs (less than 100 on account of the manual acquisition) should be less efficient to describe the whole actual field of disparities than our automatic method.

## 6. ACKNOWLEDGEMENT

Philippe Blanc has a fellowship from the Ministry of Defence (DGA/CNRS) for his Ph.D.

## REFERENCES:

Blanc, P., L. Wald and T. Ranchin, 1998. Importance and effect of co-registration quality in an example of « pixel to pixel » fusion process. In: Proceedings of the International Conference « Fusion of Earth data: merging point measurements, raster maps and remotely sensed images », Sophia Antipolis, France, 28-30 January.

Djamdj, J.P., A. Bijaoui, and R. Manière, 1993. A new method of automatic registration, based on a multiresolution decomposition of the images using the

wavelet transform. *Photogrammetric Engineering & Remote Sensing*, 59(5):645-653.

Djamdj, J.P., A. Bijaoui, 1995. Earth science and remote sensing disparity analysis and image registration of stereoscopic images using the wavelet transform. In: Proceedings of SPIE conference "Image and Signal Processing for Remote Sensing II", Paris, France, 25-27 September. 2579:11-21.

Holdshneider, M., R. Kronland-Martinet, J. Morlet and P. Tchamitchian, 1989. Wavelets: Time-frequency methods and phase-space, Chapter A: real time algorithm for signal analysis with the help of the wavelet transform. Springer Berlin. pp. 286-297.

Leclerc, V., 1987. Recalage élastique d'images angiographiques. Thèse de Docteur-Ingénieur, Ecole Nationale Supérieure des Télécommunications. ENST-87E024. 164 pp.

Lemehaute, A.J.Y., 1989. A finite approach to surface reconstruction. Université des sciences et techniques de Lille, France, 39 pp.

Moravec, H.P., 1977. Towards automatic visual obstacle avoidance. In: Proceedings of the 5th. International Joint Conference of Artificial Intelligence, Cambridge, August 1977, p 584.

Townshend, J.R.G., C.O. Justice, C. Gurney and J. McManus, 1992. The impact of misregistration on change detection, *IEEE Transactions on Geoscience and Remote Sensing*, 30(5):1054-1060.

Wald, L., T. Ranchin, and M. Mangolini, 1997. Fusion of Satellite Images of Different Spatial Resolutions: assessing the quality of resulting images. *Photogrammetric Engineering & Remote Sensing*, 63(6), pp. 691-699.

Watson, D.F., 1981. Computing the n-dimensional Delaunay tessellation with application to Voronoï polytopes. *The Computer Journal*, 24.